ORIGINAL

Radiation Medicine: Vol. 8 No. 4, 136–144 p.p., 1990

Magnetic Resonance Imaging of the Cavernous Sinus

Masaki Komiyama, M.D.*

The magnetic resonance (MR) appearance of the cavernous sinus (CS) was studied in 10 normal and 23 abnormal CSs (11 vascular and 12 neoplastic lesions) using T_1-weighted spin echo images with and without Gd-DTPA.

In normal CSs, the intracavernous carotid artery (ICA) was disclosed as an area of signal void that was not enhanced with Gd-DTPA. Most venous flow showed low intensity and was markedly enhanced with Gd-DTPA. Venous flow, however, was heterogeneous, which suggested the distribution of flow velocities.

In the carotid-cavernous sinus fistulas (CCFs), the ICA and shunted flow were disclosed as areas of signal void and their relationship was clearly shown. Normal venous flow appeared as a low intensity area even with CCFs. In the cavernous aneurysms, thrombosis and patent arterial flow were shown, but in one case it was impossible to differentiate patent arterial flow from calcification.

In neoplastic lesions, CS invasion was suspected by encasement or marked dislocation of the ICA, disappearance of venous flow, and extension of extrasellar tumors to the medial wall and extension of sellar tumors to the lateral wall.

MR was found to be a promising diagnostic modality for the evaluation of the CS.

Key words: blood flow, cavernous sinus, gadolinium-DTPA, invasion, magnetic resonance imaging

Introduction

With the advances of microneurosurgery and interventional vascular surgery, the cavernous sinus (CS) is no longer an obscure area. The CS has such a complex anatomical structure that it is usually difficult to observe both the vascular and neural structures using conventional diagnostic modalities. Arterial flow is well demonstrated by cerebral angiography; however, even with cerebral angiography and orbital and/or internal jugular venography, venous flow is not always clearly demonstrated.

The usefulness of magnetic resonance (MR) imaging for the evaluation of various lesions in the central nervous system is already well recognized. Demonstration of the intracavernous carotid artery (ICA), normal venous flow, and rapidly flowing shunted blood, if any, including the anatomical relationship with surrounding structures, is of utmost concern in patients with vascular lesions. Demonstration of the CS invasion and the relationship of the tumor to the visual pathways and the ICA is also most important in patients with neoplastic lesions. The aim of this study was to determine the usefulness of MR for the evaluation of the CS under normal and pathological conditions.

* Department of Neurosurgery, Baba Memorial Hospital. Reprint requests to Masaki Komiyama, M.D., Department of Neurosurgery, Baba Memorial Hospital, 4–244 Higashi, Hamadera Funao-Cho, Sakai, Osaka 592, JAPAN.

Materials and Methods

For the study of the normal CS, 10 normal CSs of nine supratentorial brain tumor cases (three gliomas, four meningiomas, one cavernous hemangioma, and one metastasis) and one cerebral infarction case (four males and six females, aged 20 to 79) underwent MR examination. All the patients were free of CS symptoms and the normal CSs were verified by cerebral angiography and X-ray computed tomography (CT).

MR examinations were carried out in 23 patients

with intracavernous pathologies who were divided into two groups on the basis of clinical diagnoses. One group included 11 vascular lesions: one traumatic carotid-cavernous sinus fistula (CCF), seven dural CCFs, and three large or giant aneurysms (one male and 10 females, aged 45 to 72). The other group included 12 neoplastic lesions: four meningiomas, three neurinomas, four pituitary adenomas, and a chondroma (two males and 10 females, aged 17 to 59).

The MR scanner used was a 0.5 Tesla superconductive MR system (Vista-MR, Picker International, Cleveland, Ohio, USA). Pulse sequences were T_1-weighted spin echo (SE), repetition time and echo time being 400–1,200 and 30–40 msec, respectively. Image planes were orthogonal, with a thickness of 1.0 or 0.5 cm. The field of view was 30 cm and the image matrix was 256×256; the number of slices imaged simultaneously was one, four, or eight. Data averaging was carried out once or twice. Image reconstruction was performed via two-dimensional Fourier transformation.

After scanning without contrast medium, gadolinium-diethylenetriamine pentaacetic acid (Gd-DTPA) was administered intravenously at a dose of 0.1 mmol/kg body weight within one minute in most cases. Scanning with contrast medium was performed immediately after the administration of Gd-DTPA or at least within 40 minutes. Skull X-rays, plain and enhanced CT, and cerebral angiography were performed in all cases. The diagnoses of all vascular lesions were made radiologically. The diagnoses of neoplastic lesions were made histopathologically, and invasion to the CS was verified surgically in all cases.

Results

I. Normal CS (Fig. 1)

1. Arterial flow in the CS

The ICA was always disclosed as a no-signal area in the non-contrast study and was not enhanced with Gd-DTPA (10/10 cases). The small arterial branches from the ICA were not disclosed in any patient. The ICA on coronal images was always round-shaped and no artifact was observed around the ICA attributable to arterial pulsation.

2. Venous flow in the CS

Most venous flow in the CS was disclosed as an area of low intensity, showing almost the same intensity as the cerebral cortex in the non-contrast study. This low intensity area was markedly enhanced with Gd-DTPA (10/10 cases). In the non-contrast study, however, venous flow was not always homogeneous, with several areas of higher and lower intensity noted. These areas were usually small, but there were relatively large areas with high intensity in one case and very low intensity (not an absolute void such as the ICA) in three cases. These relatively large areas with different signal intensities from those of most venous spaces were round-shaped. Very low intensity areas were also enhanced with Gd-DTPA to some degree, but not so markedly as in most venous spaces.

Fig. 1. Normal Cavernous sinus. a: T_1-weighted spin echo image (TR/TE, 600/40 msec) without Gd-DTPA. The cavernous sinus is demonstrated as a heterogeneous low intensity area (*open curved arrow*) and the internal carotid artery shows no signal intensity (*double arrows*). Note the cranial nerves: the oculomotor/trochlear nerve complex (A), the abducent nerve (B), and the first branch of the trigeminal nerve (C) at the right lateral wall of the cavernous sinus. The small *arrowheads* indicate the optic chiasm. b: Image obtained with the same pulse sequence with Gd-DTPA enhancement. The cavernous sinus as well as pituitary gland and its stalk (*arrow*) are markedly enhanced, while the internal carotid artery shows no signal. The cranial nerves at the lateral wall are not enhanced (*arrowheads*).

3. Cranial nerves in the CS

Cranial nerves were identified as areas of slightly lower intensity than most venous spaces on coronal images (4/10 cases). They were located in the lateral portion of the CSs. These cranial nerves were not enhanced with Gd-DTPA and were easily recognized in the enhanced study because the surrounding venous spaces were markedly enhanced.

II. Pathological CS

A. Vascular lesions

1. Traumatic CCF (Fig. 2)

The ICA and rapidly flowing shunted blood in the draining channels in the CS were visualized as areas of signal void, whereas the remaining venous flow, even on the ipsilateral side of the CCF, appeared as an area of low signal intensity. Gd-DTPA markedly enhanced the remaining venous flow, but did not enhance arterial flow in the ICA or shunted flow in the draining channels. The dilated superior ophthalmic vein was also visualized as an area of signal void. Although the site of the fistula was not definetely depicted by MR, the relationship between the ICA and draining channels was clearly shown on coronal images.

2. Dural CCF (Fig. 3)

According to Barrow's classification, all seven cases were type D, which meant both the external and internal carotid arteries contributed to the CCFs.[1] Feeding arteries were detected solely by angiography. Even with knowledge of the angioarchitecture as demonstrated by angiography, it was impossible to depict the feeding arteries by MR in any of the cases. With MR, the superior ophthalmic vein (SOV) was demonstrated as an area of signal void in four cases (all cases in which the SOVs were the main draining pathways). In one case, the inferior ophthalmic vein was also demonstrated as an area of signal void. In another case, the inferior petrosal sinus was demonstrated as an area of signal void by MR.

CT could not demonstrate the draining pathways because the contrast medium enhanced the whole CS in addition to the ICA. The draining pathways in the CS were demonstrated by MR in all cases as areas of very low or almost negligible signal intensity. In two cases in which patients experienced oculomotor palsy, the draining pathway was located supero-lateral or lateral to the ICA. In the other four cases, which primarily experienced abducent nerve palsy and had no or minimal oculomotor nerve palsy, this very low intensity area was located lateral or infero-lateral to the ICA. In the remaining

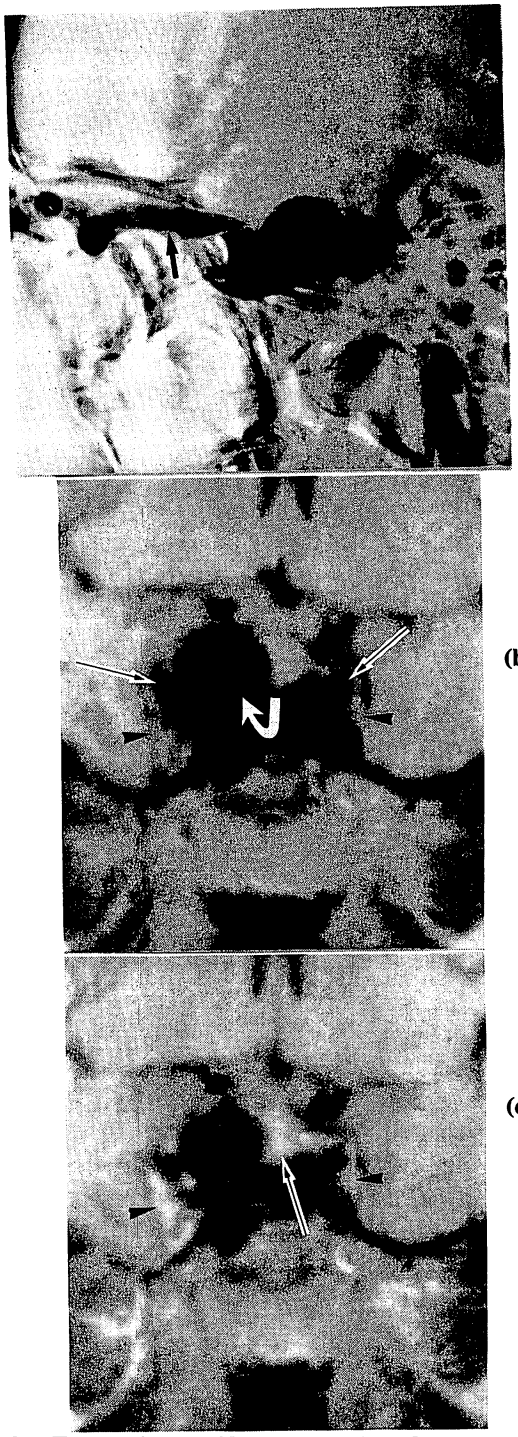

Fig. 2. Traumatic carotid-cavernous sinus fistula. a: Internal carotid injection (lateral view) shows the large high-flow shunt at the cavernous sinus. There is no visualization of the intracranial blood flow due to large shunt. The dilated cavernous sinus and superior ophthalmic vein (*arrow*) are clearly shown. However, it is unclear whether there is normal venous flow in the cavernous sinus. b: T_1-weighted spin echo image obtained without Gd-DTPA discloses the dilated venous cavity (*curved arrow*), which is located medial to the internal carotid artery, as an area of signal void due to the rapid shunted flow. *Arrows* indicate the internal carotid artery. Low intensity areas representing the normal venous flow are noted even where the arteriovenous fistula coexists (*arrowheads*). c: Enhanced image with Gd-DTPA shows that the normal venous flow and pituitary gland (*arrow*) are markedly enhanced. The arterial flow in the internal carotid artery and the draining venous pathway are demonstrated as areas of signal void.

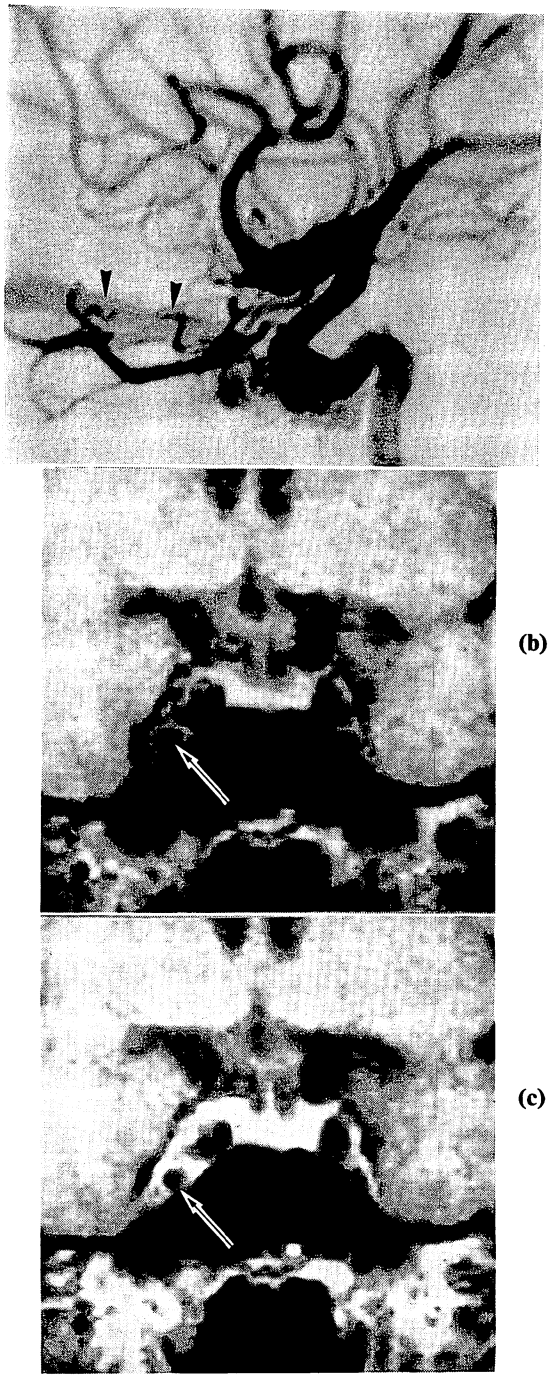

Fig. 3. Dural carotid-cavernous sinus fistula. a: Internal carotid injection (lateral view) shows the shunted flow, which is located inferior to the carotid artery and is draining to the superior ophthalmic vein (*arrowheads*). b: T_1-weighted spin echo image obtained without Gd-DTPA shows the draining pathway (*arrow*), which is located infero-lateral to the internal carotid artery. This shunted flow is demonstrated as an area of signal void similar to carotid flow. c: Enhanced image with Gd-DTPA shows that normal venous flow in the cavernous sinus is markedly enhanced, but the shunted flow remains an area of signal void (*arrow*).

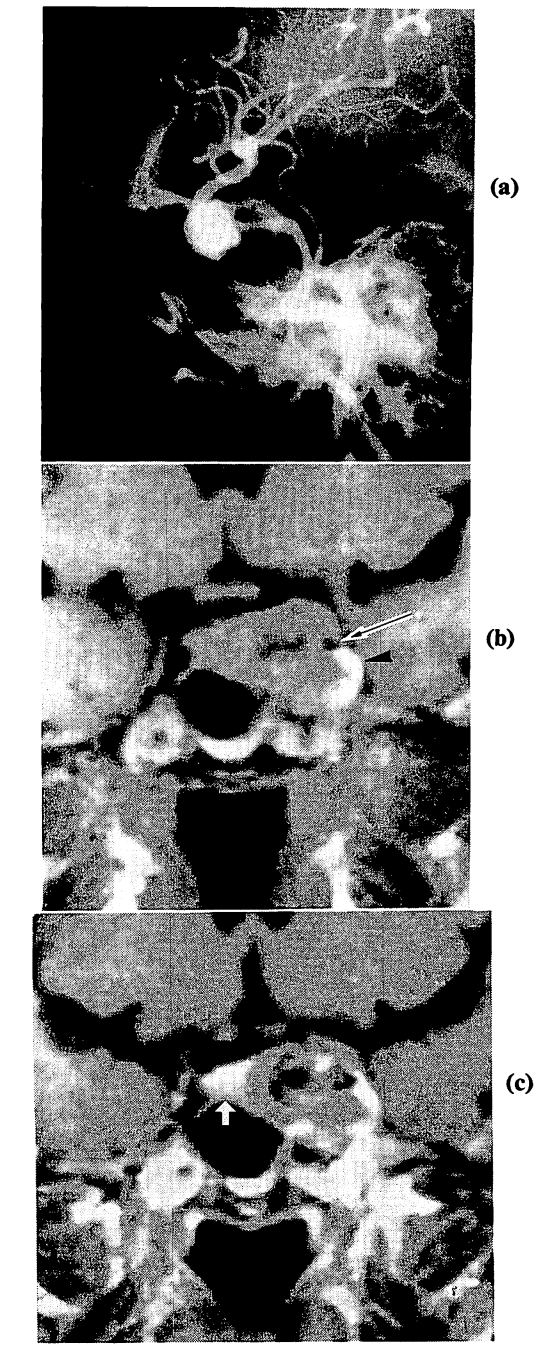

Fig. 4. Partially thrombosed giant aneurysm. a: Common carotid injection shows an aneurysm at the cavernous sinus. It is not clear whether there is a thrombosis in the aneurysmal lumen. b: Plain MR image shows the small patent arterial flow as an area of signal void (*arrow*). The thrombosis exhibits heterogeneous signal intensity. The relationship between the thrombosis, the patent arterial flow, and the optic chiasm is clearly shown. The small high intensity area at the lateral wall of the aneurysm is probably caused by methemoglobin within the thrombosis (*arrowhead*). c: Image enhanced with Gd-DTPA shows the enhanced pituitary gland (*arrow*), while the patent carotid flow is an area of signal void. The aneurysmal lumen shows heterogeneous intensity.

case, in which the patient had full extraocular movement, this area was located mainly medial to the ICA. These draining pathways were clearer on coronal images than on sagittal images. No thrombosis in the CS or SOV, which would have shown up as an area of high intensity on the T_1-weighted SE images, was noted in this series.

Only MR was able to demonstrate normal venous pathways abutting abnormal venous pathways, in which shunted blood flowed. These normal venous pathways were heterogeneous in intensity, but generally had a low signal intensity that was slightly higher than the intensity of abnormal shunted blood. These normal pathways were markedly enhanced by Gd-DTPA, allowing easy recognition of the venous compartments.

3. Large or giant aneurysms (Fig. 4)

In one case of thrombosed aneurysm, patent arterial flow in the thrombosis was disclosed as an area of signal void and a thrombosed clot was visualized as a low intensity area with an intensity similar to that of the cerebral cortex. The CS was almost obliterated by the clot, leaving a small residual venous space at the lateral wall of the thrombosed aneurysm. This residual venous space was markedly enhanced by Gd-DTPA. In another case with calcification and thrombosis, the wall of the aneurysm showed no signal, which correlated with the calcification depicted by CT. Small patent arterial flow was not clearly depicted by MR since it was too small, with the calcification located very near to it showing similar intensity. The CS was completely obliterated by the thrombosis, leaving no venous flow. The clot had two different intensities, one the same as the cerebral cortex and the other much lower. In a case without thrombosis, the large intra-aneurysmal cavity was demonstrated as an area of signal void.

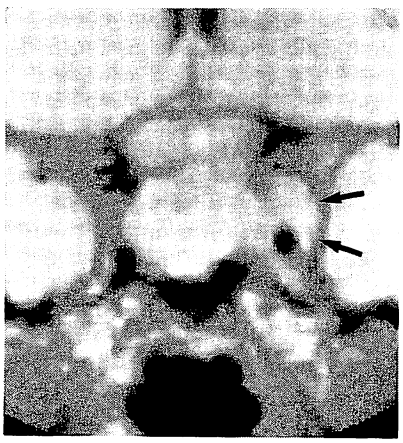

Fig. 5. Pituitary adenoma. The invasion to the left cavernous sinus (*arrows*) is surgically verified. The low intensity area representing normal venous flow has completely disappeared. The internal carotid artery is completely encased by the tumor. The tumor extends to the lateral wall of the cavernous sinus.

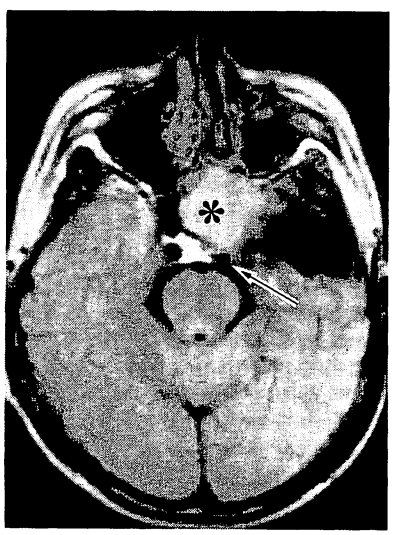

Fig. 6. Meningioma at the right sphenoidal ridge. The internal carotid artery (*arrow*) is displaced posteriorly by the recurrent tumor (*asterisk*), and the right cavernous sinus is completely obliterated by the tumor.

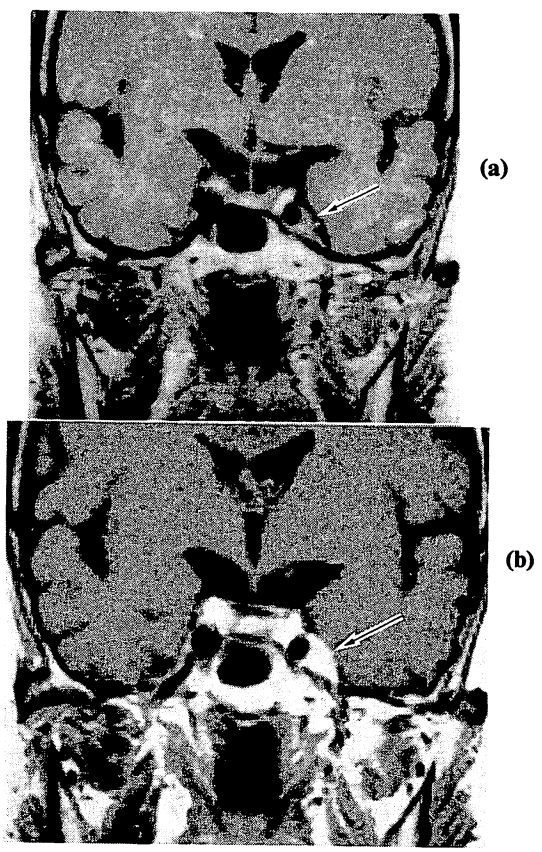

Fig. 7. Neurinoma of the trigeminal nerve. a: Plain MR image shows bulging of the left lateral wall of the cavernous sinus (*arrow*). b: Image enhanced with Gd-DTPA shows the enhanced mass (*arrow*) in the left cavernous sinus. The tumor is attached to the internal carotid artery.

After proximal balloon occlusion of the ICA, stasis of blood flow within the cavity was observed with MR.

B. Neoplastic lesions (Figs. 5–7)

All tumors showed almost the same intensity as the cerebral cortex or slightly lower. The relationship between the visual pathways and the tumors was usually clearly depicted unless the visual pathways were involved in the tumors or were markedly compressed. The relationship between the ICA, anterior and middle cerebral arteries, and tumors was also clearly shown because arterial flow always appeared as an area of signal void. Bony changes could not be demonstrated by MR, but were readily shown by CT.

Of 12 neoplastic lesions, encasement of the ICA by the tumor was recognized in seven cases. Marked dislocation of the ICA was noted in six cases. Disappearance of the low signal intensity of normal venous flow in the invaded CS was recognized in all cases but one (chondroma). This was usually observed on coronal images but was difficult to see on axial or sagittal images. Extension of intrasellar tumors to the lateral wall was noted in four cases (all of which were pituitary adenomas), and extension of extra-sellar tumors to the medial wall was noted in four cases.

Discussion

The increasing opportunities for direct surgical intervention and interventional vascular surgery in the CS necessitates precise knowledge of the CS, not only of its anatomy but also of flow within it. The structure of the CS is different from that of other cerebral venous sinuses, such as the superior sagittal, transverse, and sigmoid sinuses. It contains the ICA and the neural structures, and there are many influxes and effluxes of the venous channels connecting the CS. Although the anatomy of the CS has been extensively studied by many researchers, venous flow within it is not fully understood.[2–8] Most of the studies on the CS have been conducted with cadavers. A cadaver study makes it difficult to recognize venous spaces because they are often collapsed and filled with clots.

Understanding the signal intensity of blood flow in the CS is not straightforward because the complex anatomy of the CS and flow phenomena of MR make interpretation of this region more difficult.[9] There are basically two flow-related phenomena in MR: 1) paradoxical enhancement (flow-related enhancement and even-echo rephasing) and 2) high velocity signal loss.[10–13] Paradoxical enhancement is present in slow flow, whereas high velocity signal loss is demonstrated in rapidly flowing blood.

I. Normal CS

On T_1-weighted SE images, arterial blood flow in the ICA is always visualized as an area of signal void due to high velocity signal loss. Gd-DTPA does not increase the signal intensity because of its rapidity. Most venous flow in the CS is demonstrated in noncontrast studies as areas of low signal intensity, almost the same as the cerebral cortex, not as areas of absolute signal void.[9,14] Static blood flow shows low signal intensity and the intensity of flowing blood in the venous spaces increases or decreases depending on flow velocity and scanning parameters. However, venous flow did not show absolutely no signal like arterial flow because its velocity was less. These results are contrary to those of Daniels *et al.*, who stated that flowing blood in the CS produced negligible signals.[15] In the SE sequences used in the present study, only the first echo was used for image reconstruction. Thus, even-echo rephasing never occurred. Interestingly, venous flow was usually markedly enhanced with Gd-DTPA, unlike arterial flow. This may be attributable to the "proton relaxation enhancement" of gadolinium ions (Gd^{3+}), which produces a local magnetic field and shortens the relaxation times (T_1 and T_2) of neighboring protons.[16,17] Gd-DTPA was useful for the identification of venous spaces because enhanced areas in the CS could be identified as venous spaces, not neural structures nor fat tissues.

It is possible that the areas with intensities higher than most venous spaces represented either slowly flowing blood enhanced due to flow-related enhancement, or fat tissues.[18] Fat tissue was demonstrated in the normal CS by metrizamide CT cisternography or enhanced CT when scanned with thin-slice sections (1.5 mm).[19,20] However, it was not demonstrated in this series, probably because of the thicker slice sections (8 mm). Fat tissue has relatively short T_1 and T_2 values and shows high intensity on T_1-weighted SE images. Furthermore, images of fat shift in the direction of the lower frequency-encoding gradient due to "chemical shift" even at intermediate field when images are reconstructed via two-dimensional Fourier transformation. It is possible that some of these images were of fat tissues, but it is thought that these higher intensity areas were attributable to slowly flowing blood, the velocity of which produced higher intensity areas than the other

venous spaces, because CT revealed no fat tissue and chemical shift could not be identified in the present cases.

As for the areas with lower intensity than most venous spaces, it is possible that these represented rapidly flowing venous blood, cranial nerves, turbulent flow, or turbulence caused by transmitted pulsation from the adjacent ICA. Cranial nerves were easily identified because they were small, round-shaped, and located at the lateral portion of the CS. Further, Gd-DTPA did not enhance these structures. The complicated structure of the CS and its many influxes and effluxes can create turbulent venous flow, which causes loss of intensity due to the increased random motion of protons. The pulsation of the ICA can also cause turbulence of venous flow around the ICA. Because these areas did not always abut or surround the ICA, it is not likely that these areas were produced by transmitted pulsation from the ICA. And because the shapes of the relatively large areas with very low intensity on coronal images in two normal CSs were almost round, it is also unlikely that these were caused by turbulent flow. Although it is possible that some of them were turbulent, it is thought that these areas represented rapidly flowing blood, except the laterally located cranial nerves. Gd-DTPA enhanced these areas of rapidly flowing blood less than most venous spaces. It was thought that the velocity of this venous flow was less than that of arterial flow but more than that of most venous flow. Thus, the heterogeneous pattern of intensity of the venous spaces of the CS suggested the distribution of the velocity of venous flow. Furthermore, there was a variety of sizes of venous channels in the CS. These findings support the idea that the CS is the plexus of many veins.[21]

II-A. Vascular lesions

Traumatic CCF is caused by tearing of the ICA due to trauma. This results in a direct connection between the ICA and the CS. In traumatic CCF in this series, cerebral angiography clearly demonstrated draining channels in the CS. However, angiography sometimes fails to demonstrate the site of the fistula itself. MR clearly showed the ICA, the dilated draining channels, and their relationship.

Dural CCFs are abnormal fistulous connections between the dural branches of the internal and/or external carotid arteries and the CS.[22] Drainage is mostly through the superior and/or inferior ophthalmic veins, the inferior and/or superior petrosal sinuses, the intercavernous veins and the basilar plexus draining into the opposite CS, and the pterygoid plexus. Sometimes drainage is to the cortical veins. In dural CCFs, MR also clearly demonstrates shunted flow in the CS and the SOV as areas of signal void due to high velocity signal loss.[23,24]

Mullan divides the CS into two cavities: a larger antero-inferior portion and a smaller postero-superior portion by the ICA.[25] He reported that in CCF distension of a main channel presumably obliterates lesser channels and these two cavities might connect freely, forming only a single cavity, or they may occasionally remain separate. Harris and Rhoton reported that the three major venous spaces within the CS were postero-superior, antero-inferior, and medial to the cavernous portion of the ICA, and they appeared to be largely unbroken trabeculated venous channels.[4] Contrary to their observations, venous channels which had no relation to the CCF were clearly demonstrated by MR, and this was confirmed by enhanced MR with Gd-DTPA. These venous channels probably had slow flowing blood, even if CCFs existed. This observation again supports Parkinson's idea that the CS is a plexus of various-sized venous channels.[21] With regard to CCF, it can be inferred that one venous channel is markedly dilated with shunted flow, whereas the remaining channels, which have no direct connection with the CCF, have normal venous flow. Non-shunted blood flow has not been acceptably demonstrated by conventional diagnostic modalities. MR provided clear, separate disclosure of shunted and non-shunted blood flow.

From an anatomical point of view, the oculomotor nerve in the CS is located supero-lateral to the ICA, and the abducent nerve is lateral to the ICA on the coronal plane.[8] In our dural CCFs, oculomotor nerve palsy with partial abducent palsy was noted in one case and abducent nerve palsy was predominantly noted in the other four cases. The signal void in the CS demonstrated on coronal images was inevitably located near the paralyzed nerves, with a lateral or infero-lateral location for abducent nerve palsy and supero-lateral location for oculomotor nerve palsy. The real reason for nerve palsy is unknown, but MR observation suggests that mechanical compression of the nerve by shunted blood is more likely than ischemia of the nerve due to increased venous pressure.

The etiology of dural CCF is not well understood. Newton and Hoyt thought "rupture of the small dural branch" that travels through the CS to be the cause of dural CCF.[22] On the other hand, the angiographic features of abnormal venous drainage

patterns in the CS, filling defects within the CS and its tributaries, the abnormal shape of the CS, and venous stasis indirectly suggest "thrombosis formation" in the CS.[26] MR demonstrates venous thrombosis as an area of high intensity on both T_1- and T_2-weighted SE images.[29] Sergott *et al.* reported dural CCF with thrombosis formation in the SOV depicted by MR, but not in the CS.[28] Since no thrombosis formation in the CS was detected in our series, we think that further examination is necessary to determine the role of thrombosis formation in the CS as a possible cause of dural CCF.

Aneurysm is usually recognized by MR as a dilated vascular cavity connected to the normal vascular anatomy. It appears as an area of signal void due to high velocity signal loss, but paradoxical enhancement may occur in the case of slow flow.[29,30] Thrombosis must be differentiated from neoplasms, but this is sometimes difficult. Methemoglobin and hemosiderin in the thrombosis show peculiar intensities, appearing as high and low intensity areas, respectively.[29] This may contribute to the differentiation of aneurysms from neoplastic lesions. In one of our cases, part of the thrombosis showed very low intensity, probably due to hemosiderin. Residual venous flow in a CS almost obliterated by an aneurysm (rarely demonstrable with cerebral angiography) could be demonstrated in a case of giant thrombosed aneurysm. This small venous flow was markedly enhanced with Gd-DTPA. Flow change after intraluminal proximal balloon occlusion of the ICA clearly demonstrated in another case.

II-B. Neoplastic lesions

MR was excellent in defining the relationship of the tumor to the ICA, pituitary gland, and optic nerves and chiasm.[30,31] Although MR cannot provide detailed tissue characterization of brain tumors and T_1-weighted SE images cannot provide high tissue contrast between the tumor and normal tissue, T_1-weighted SE images are suitable for study of the CS because of their high spatial resolution.[31,32] Due to this relative lack of tissue contrast of T_1-weighted SE images, all tumors in this study showed almost the same intensity as the cerebral cortex. However, it is important to determine whether the tumor is invading the CS or not, since CS invasion sometimes changes the therapeutic plan from radical surgery to palliative radiation. Kline *et al.* reported that the following CT characteristics suggest an abnormal CS: (1) asymmetry of size, (2) asymmetry of shape, particularly the lateral wall, and (3) focal areas of abnormal density within the CS.[33] Ahmadi *et al.* reported that indications of CS invasion by pituitary adenomas were (1) CS expansion, (2) visible encasement of the ICA, (3) compression or displacement of the intracavernous cranial nerves, (4) invasion of the lateral wall, and (5) diffuse bony destruction.[34]

When the tumor completely encases the ICA, invasion of the CS is obvious. However, complete encasement of the ICA is not always necessary for diagnosing invasion of the CS. We found four MR signs suggestive of CS invasion: (1) encasement (partial or complete) of the ICA, (2) marked dislocation of the ICA, (3) disappearance of low signal intensity representing normal venous flow in the CS, which is markedly enhanced with Gd-DTPA, and (4) extension of intra-sellar tumors to the lateral wall or extension of extra-sellar tumors to the medial wall.[35] Except for disappearance of the low intensity of normal venous flow, the above-mentioned signs hold true in CT. Scotti *et al.* reported similar results, i.e., that MR signs of CS invasion by pituitary adenomas were the presence of unilateral CS enlargement and signal-intensity changes or the presence of ICA encasement.[18] The lack of artifacts from adjacent bone is one advantage of MR, since CT images of the CS are always degraded by streak artifacts and coronal images can be obtained only with the patient's cooperation. Since the intracavernous cranial nerves were not always visualized with our MR system, we could not use involvement of the cranial nerves as a criterion for determining CS invasion. With the further improvement of MR technology, involvement of the cranial nerves will also serve as a useful indicator for CS invasion.

In conclusion, we found that MR could give far more detailed anatomical and flow information on the CS than conventional diagnostic modalities, including CT. Our experiences encourage the further use of MR in this field.

ACKNOWLEDGMENTS

This work has been partially presented at (1) the International Symposium on Cavernous Sinus, Ljubljana, Yugoslavia, June 1986, (2) the 8th European Congress of Neurosurgery, Barcelona, Spain, September 1987, (3) the 13th annual meeting of the Japanese Society of Brain CT, Okayama, January 1990, (4) International Symposium on Processes of the Cranial Midline, Vienna, Austria, May 1990, and (5) the 2nd annual meeting of the Japanese Society for Skull Base Surgery, Osaka, July 1990.

The author is grateful to Drs. A. Hakuba and S. Nishimura, Department of Neurosurgery, Osaka City University Medical School, for their encouragement to carry out this work and their valuable advice.

References

1) Barrow DL, Spector RH, Braun IF, Landman JA, Tindall SC, Tindall GT. Classification and treatment of spontaneous carotid-cavernous sinus fistulas. *J Neurosurg*, 62: 248–256, 1985.
2) Parkinson D. Collateral circulation of cavernous carotid artery: anatomy. *Can J Surg*, 7: 251–268, 1964.
3) Bedford MA. The "cavernous" sinus. *Brit J Ophthal.* 50: 41–46, 1966.
4) Harris FS, Rhoton AL Jr. Anatomy of the cavernous sinus. A microsurgical study. *J Neurosurg*, 45: 169–180, 1976.
5) McGrath P. The cavernous sinus: an anatomical survey. *Aust NZ J Surg*, 47: 601–613, 1977.
6) Miyazaki H. The "cavernous" sinus. *Neurol Surg (Tokyo)*, 9: 1131–1138, 1981.
7) Taptas JN. The so-called cavernous sinus: A review of the controversy and its implications for neurosurgeons. *Neurosurgery*, 11: 712–717, 1982.
8) Umansky F, Nathan H. The lateral wall of the cavernous sinus. With special reference to the nerves related to it. *J Neurosurg*, 56: 228–234, 1982.
9) Komiyama M, Yasui T, Baba M, Hakuba A, Nishimura S, Inoue Y. MR imaging of blood flows in the cavernous sinus. *Radiat Med*, 6: 124–129, 1988.
10) Mills CM, Brant-Zawadzki M, Crooks LE, *et al.* Nuclear magnetic resonance: principles of blood flow imaging. *AJR*, 142: 165–170, 1984.
11) Bradley WG, Waluch V, Lai K-S, Fernandez EJ, Spalter C. The appearance of rapidly flowing blood on magnetic resonance images. *AJR*, 143: 1167–1174, 1984.
12) Bradley WG, Jr, Waluch V. Blood flow: magnetic resonance imaging. *Radiology*, 154: 443–450, 1985.
13) Kucharczyk W, Kelly WM, Davis DO, Norman D, Newton TH. Intracranial lesions: flow-related enhancement on MR images using time-of-flight effects. *Radiology*, 161: 767–772, 1986.
14) Komiyama M, Yasui T, Baba M, *et al.* MR imaging: normal and invaded cavernous sinus studied with and without Gd-DTPA. In *The Cavernous Sinus* (Dolenc VV eds.; Springer-Verlag, Vienna, New York), pp. 152–161, 1987.
15) Daniels DL, Pech P, Mark L, *et al.* Magnetic resonance imaging of the cavernous sinus. *AJNR*, 6: 187–192, 1985.
16) Runge VM, Clanton JA, Lukehart CM, Partain CL, James AE Jr. Paramagnetic agent for contrast-enhanced NMR imaging: a review. *AJR*, 141: 1209–1215, 1983.
17) Carr DH, Brown J, Leung A W-L, Pennock JM. Iron and gadolinium chelates as contrast agents in NMR imaging: preliminary studies. *J Comput Assist Tomogr*, 8: 385–389, 1984.
18) Scotti G, Yu C-Y, Dillon WP, *et al.* MR imaging of cavernous sinus involvement by pituitary adenomas. *AJR*, 151: 799–806, 1988.
19) Hosoya T, Kera M, Suzuki T, Yamaguchi K. Fat in the normal cavernous sinus. *Neuroradiology*, 28: 264–266, 1986.
20) Stricof DD, Gabrielsen TO, Latack JT, Gebarski SS, Chandler WF. CT demonstration of cavernous sinus fat. *AJNR*, 10: 1199–1201, 1989.
21) Parkinson D. Carotid cavernous fistula: direct repair with preservation of the carotid artery. Technical note. *J Neurosurg*, 38: 99–106, 1973.
22) Newton TH, Hoyt WF. Dural arteriovenous shunts in the region of the cavernous sinus. *Neuroradiology*, 1: 71–81, 1970.
23) Hirabuki N, Miura T, Mitomo M, *et al.* MR imaging of dural arteriovenous malformations with ocular signs. *Neuroradiology*, 30: 390–394, 1988.
24) Komiyama M, Fu Y, Yagura H, Yasui T, Hakuba A, Nishimura S. Imaging of dural AV fistulas at the cavernous sinus. *J Comput Assist Tomogr*, 14: 397–401, 1990.
25) Mullan S. Treatment of carotid-cavernous fistulas by cavernous sinus occlusion. *J Neurosurg*, 50: 131–144, 1979.
26) Seeger JF, Gabrielsen TO, Giannotta SL, Lotz PR. Carotid-cavernous sinus fistulas and venous thrombosis. *AJNR*, 1: 141–148, 1980.
27) McMurdo SK, Jr, Brant-Zawadzki M, Bradley WG Jr, Chang GY, Berg BO. Dural sinus thrombosis: study using intermediate field strength MR imaging. *Radiology*, 161: 83–86, 1986.
28) Sergott RC, Grossman RI, Savino PJ, Bosley TM, Schatz NJ. The syndrome of paradoxical worsening of dural-cavernous sinus arteriovenous malformations. *Ophthalmology*, 94: 205–212, 1987.
29) Atlas SW, Grossman RI, Goldberg HI, Hackney DB, Bilaniuk LT, Zimmerman RA. Partially thrombosed giant intracranial aneurysms: correlation of MR and pathological findings. *Radiology*, 162: 111–114, 1987.
30) Hirsch WL Jr, Hryshko FG, Sekhar LN, *et al.* Comparison of MR imaging, CT, and angiography in the evaluation of the enlarged cavernous sinus. *AJR*, 151: 1015–1023, 1988.
31) Komiyama M, Fu Y, Yagura H, *et al.* Magnetic resonance imaging of pituitary adenomas. *Neurol Med Chir (Tokyo)*, 27: 733–737, 1987.
32) Komiyama M, Yagura H, Baba M, *et al.* MR imaging: possibility of tissue characterization of brain tumors using T_1 and T_2 values. *AJNR*, 8: 65–70, 1987.
33) Kline LB, Acker JD, Post MJD, Vitek JJ. The cavernous sinus: a computed tomographic study. *AJNR*, 2: 299–305, 1981.
34) Ahmadi J, North CM, Segall HD, Zee C-S, Weiss MH. Cavernous sinus invasion by pituitary adenomas. *AJNR*, 6: 893–898, 1985.
35) Komiyama M, Hakuba A, Yasui T, *et al.* Magnetic resonance imaging of intracavernous pathology. *Neurol Med Chir (Tokyo)*, 29: 573–578, 1989.